Skeletal Radiology (2023) 52:2069–2083
https://doi.org/10.1007/s00256-023-04422-4

REVIEW ARTICLE

Subchondral bone in knee osteoarthritis: bystander or treatment target?

Arta Kasaeian[1] · Frank W. Roemer[2,3] · Elena Ghotbi[1] · Hamza Ahmed Ibad[1] · Jianwei He[4] · Mei Wan[4] · Wojciech B. Zbijewski[5] · Ali Guermazi[2] · Shadpour Demehri[1]

Received: 14 November 2022 / Revised: 1 August 2023 / Accepted: 1 August 2023 / Published online: 30 August 2023

Abstract

The subchondral bone is an important structural component of the knee joint relevant for osteoarthritis (OA) incidence and progression once disease is established. Experimental studies have demonstrated that subchondral bone changes are not simply the result of altered biomechanics, i.e., pathologic loading. In fact, subchondral bone alterations have an impact on joint homeostasis leading to articular cartilage loss already early in the disease process. This narrative review aims to summarize the available and emerging imaging techniques used to evaluate knee OA-related subchondral bone changes and their potential role in clinical trials of disease-modifying OA drugs (DMOADs). Radiographic fractal signature analysis has been used to quantify OA-associated changes in subchondral texture and integrity. Cross-sectional modalities such as cone-beam computed tomography (CT), contrast-enhanced cone beam CT, and micro-CT can also provide high-resolution imaging of the subchondral trabecular morphometry. Magnetic resonance imaging (MRI) has been the most commonly used advanced imaging modality to evaluate OA-related subchondral bone changes such as bone marrow lesions and altered trabecular bone texture. Dual-energy X-ray absorptiometry can provide insight into OA-related changes in periarticular subchondral bone mineral density. Positron emission tomography, using physiological biomarkers of subchondral bone regeneration, has provided additional insight into OA pathogenesis. Finally, artificial intelligence algorithms have been developed to automate some of the above subchondral bone measurements. This paper will particularly focus on semiquantitative methods for assessing bone marrow lesions and their utility in identifying subjects at risk of symptomatic and structural OA progression, and evaluating treatment responses in DMOAD clinical trials.

Keywords Osteoarthritis · Disease-modifying OA drugs · Magnetic resonance imaging · Bone marrow lesions

Introduction

Knee osteoarthritis (OA) is a complex and progressive disease. It may evolve over several decades and, if left untreated, ultimately leads to knee replacement surgery. The burden of knee OA on healthcare services is expected to increase with improvements in global life expectancy [1–4].

Non-pharmacological interventions such as weight loss, physiotherapy, and joint replacement have been the main treatment options in routine clinical practice for knee OA management. Currently, no disease-modifying medication (DMOAD) for OA has been approved by regulatory authorities. DMOADs are groups of pharmacological therapies investigated for their protective or restoring effects on articular cartilage, reducing inflammation, and impacting subchondral bone changes to stop or delay structural progression [5, 6].

✉ Shadpour Demehri
demehri2001@yahoo.com

1 Musculoskeletal Radiology, Russell H. Morgan Department of Radiology and Radiological Science, Johns Hopkins University School of Medicine, Baltimore, MD, USA

2 Department of Radiology, Boston University School of Medicine, Boston, MA, USA

3 Department of Radiology, University of Erlangen-Nuremberg, Erlangen, Germany

4 Department of Orthopedic Surgery, Johns Hopkins University School of Medicine, Baltimore, MD, USA

5 Department of Biomedical Engineering, Johns Hopkins University, Baltimore, MD, USA

Several articular and periarticular tissues, such as articular cartilage, synovium, periarticular muscles, menisci, and subchondral bone, contribute to disease incidence and progression. The subchondral bone comprises the subchondral bone plate, the underlying trabecular bone, and the bone marrow space. In addition, a zone of calcified cartilage separates the subchondral bone plate (composed of cortical bone) from the articular cartilage [7–10] (Fig. 1).

Biomechanical derangements such as malalignment result in altered load transfer on cartilage and the subchondral bone and will accelerate the progression of knee OA [8]. One study has shown that homeostasis and integrity of articular cartilage depend on both its biochemical and biomechanical interactions with the subchondral bone [11]. Biomechanically, early subchondral bone alterations may result in reduced shock absorption capability and, therefore, predispose the knee joint to accelerated cartilage loss. This may explain why subchondral bone trabecular morphometry measurements and subchondral bone mineral density (i.e., local periarticular BMD) changes begin early in the cascade of events, even before articular cartilage loss [12–15].

Furthermore, bone marrow lesions (BMLs) play a vital role in the detection and progression of OA, which is detected in both pre-clinical [16] and clinical knee OA [17, 18] using magnetic resonance imaging (MRI) examinations. MRI also allows for the noninvasive detection and characterization of longitudinal subchondral bone changes at an early stage in the development of knee OA [19]. These changes include disruption of trabecular connectivity, trabecular microfracture, increased porosity of the subchondral bone plate, decreased trabecular thickness, decreased subchondral bone volume to total volume ratio, and resorptive changes in the subchondral bone [20–22]. Therefore, there has been tremendous recent interest in detecting OA-related subchondral bone changes at early (i.e., preclinical) stages before cartilage loss is apparent to timely implement secondary preventive measures.

The focus of this narrative review is to give an overview of available and emerging imaging techniques to detect and characterize knee OA-related changes in the subchondral bone (Table 1), with a special focus on subchondral bone biomarkers that have been investigated for the assessment of DMOAD effects of various medications in clinical trials and observational studies.

Subchondral bone in knee OA pathogenesis: brief overview of experimental evidence

There is still a lack of knowledge regarding the complex interactions between cartilage and subchondral bone during knee OA pathogenesis. The small molecules, growth factors, and cytokine pathways are involved locally in OA development and progression that could be potential treatment targets [23]. Results from animal models have revealed that there are distinct subchondral bone phenotypes in post-traumatic OA (PTOA) versus metabolic syndrome-associated OA (MetS-OA). In PTOA, subchondral bone

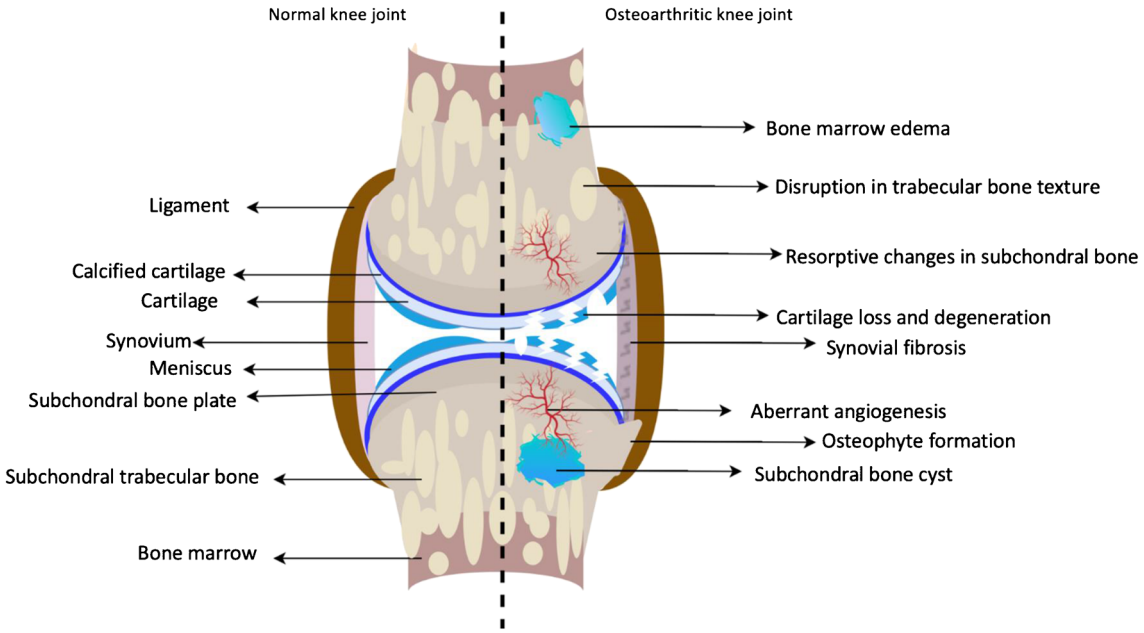

Fig. 1 Schematic illustration of normal and osteoarthritis knee joint and subchondral bone. Subchondral bone comprises the subchondral bone plate, the underlying trabecular bone, and the bone marrow. A zone of calcified cartilage separates the subchondral bone plate from the articular cartilage

Table 1 Summarizing different imaging techniques discussed and their potential uses for predicting or evaluating OA with special focus on the subchondral bone

Imaging technique	Use in evaluation and/or prediction of Osteoarthritis (OA)
Radiography	• FSA is a technique that analyzes a detailed subchondral bone architecture using any conventional plain radiograph • FSA is based on the number, spacing, and cross-connectivity of bone trabeculae • FSA of the subchondral bone has shown to be able to predict MRI measures of OA progression in human studies
CT	• MSK CBCT has shown to be superior to MDCT in image quality of knee examinations for bone visualization tasks, including trabecular pattern of medullary bone, cortical bone, and fractures detection, approaching micro-CT in human studies • MSK CBCT has demonstrated improved sensitivity and accuracy compared to radiography for the detection of subchondral cysts • CBCT allows for simultaneous assessment of joint space narrowing and subchondral bone measures in weight-bearing mode • CE-CBCT can be used to obtain volumetric bone mineral density measurements in cadaveric specimens and in vivo studies • Micro CT imaging has proven to be effective in visualizing alterations in subchondral bone microarchitecture in experimental studies investigating the potential DMOAD role for various medications
MRI	• The MRI Osteoarthritis Knee Score (MOAKS) is a validated scoring system used to measure subchondral bone marrow lesions and other OA-related structural damages (cartilage, menisci, ext.) • MRI and the MOAKS have been successfully employed to assess the structural damages in subchondral bone resulting from the application of various DMOADs in human studies • High-resolution 3D fast MRI with free steady-state precession (FISP) sequences have been used to assess subchondral bone texture and periarticular bone biomarkers such as trabecular bone volume fraction, number, thickness, and spacing
DEXA	• Exact association pattern and underlying mediatory factors between DEXA-derived systemic and local BMD and the incidence/progression of OA remain unclear • Further research is needed to understand the mechanisms underlying subchondral BMD changes in knee osteoarthritis
PET	• Hybrid PET-MRI systems using MOAKS have also identified biomarkers of OA progression in early knee OA patients
Artificial intelligence	• AI has shown to be a promising tool for automated detection of microstructural changes in the subchondral bone using various imaging modalities and may be used to assess therapeutic effect of DMOADs in future clinical trials

FSA fractal signature analysis, *MSK* musculoskeletal, *CBCT* cone-beam computed tomography, *MDCT* multidetector CT, *CE-CBCT* contrast-enhanced CBCT, *DEXA* dual-energy X-ray absorptiometry, *PET* positron emission tomography, *BMD* bone mineral density

changes have shown a biphasic nature in disease progression. In the early stages of OA, subchondral bone osteoclast bone remodeling and loss of osseous trabeculations are dominant. In later stages, subchondral bone sclerosis and osteophyte growth become prominent (Fig. 2A) [22, 24–26]. On the other hand, there is rapid subchondral bone trabecular growth and, consequently, thickening of the subchondral bone plate and trabecular bone in MetS-OA mouse models [27]. These subchondral bone alterations appear much earlier than the occurrence of cartilage degeneration. Moreover, unlike the accumulated senescent cells in cartilage and synovium in PTOA, increased senescent cells are primarily found in the subchondral bone in MetS-OA models. They secrete cytokines and proinflammatory factors to influence the subchondral bone microenvironment in MetS-OA (Fig. 2B) [28, 29].

Recent evidence has suggested an upregulated signaling and increased concentration of transforming growth factor-β1 (TGF-β1) in the subchondral bone of animal models and human knee OA (Fig. 2A). The TGF-β1 antibody stabilizes subchondral bone architecture based on micro-CT (μCT) and micro-MRI (μMRI) results in animal models and thus could serve as a potential treatment target of OA [22, 30]. Canonical Wnt pathway activation, transferring signals between the cartilage and bone, can occur in subchondral bone and osteophytes after OA incidence and in parallel with subchondral bone growth according to μCT results in mice, and inhibition of this pathway ameliorates OA severity [31, 32]. Moreover, it has been shown that preosteoclasts in osteoarthritic subchondral bone express high levels of platelet-derived growth factor-BB (PDGF-BB), which triggers neovascularization of the subchondral bone, and that joint degeneration is attenuated by PDGF-BB knockout in animal models (Fig. 2A) [25].

These observed changes in the biochemical microenvironment of subchondral bone during early OA suggest that alterations of imaging biomarkers of subchondral bone could play a critical role in detecting knee OA at an early stage in the clinical setting as well as in the mitigation of its progression [18]. In other words, there is a gradual shift from a cartilage-centric paradigm to a broader perspective focusing on the subchondral bone regarding imaging and therapeutic approaches.

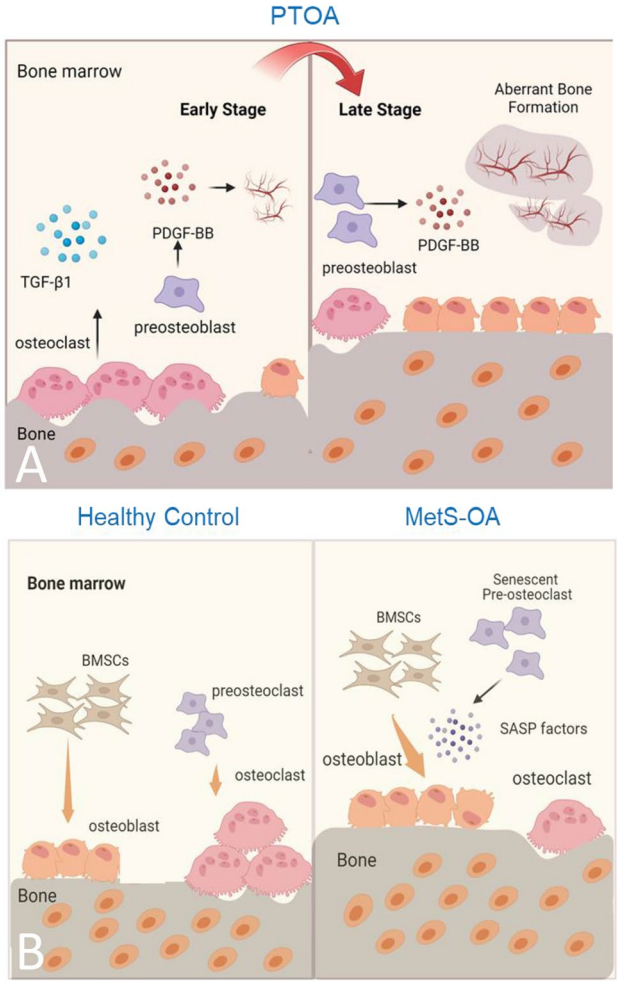

Fig. 2 Schematic illustration of osteoarthritis-related subchondral bone alterations: **A** Post-traumatic OA (PTOA). In early-stage PTOA, increased platelet-derived growth factor-BB (PDGF-BB), and active transforming growth factor beta (TGFβ) in marrow microenvironment initiate aberrant angiogenesis coupled with osteogenesis. In late-stage PTOA, aberrant bone formation and neo-vessel invasion into cartilage lead to articular cartilage ossification and joint degeneration. **B** Metabolic syndrome-associated osteoarthritis (MetS-OA). Under metabolic stress, preosteoclasts in the subchondral bone marrow undergo cellular senescence and secrete senescence-associated secretory phenotype (SASP) factors, which promote osteoblast differentiation and inhibit osteoclast differentiation for a rapid thickening of the subchondral plate and trabecular bone

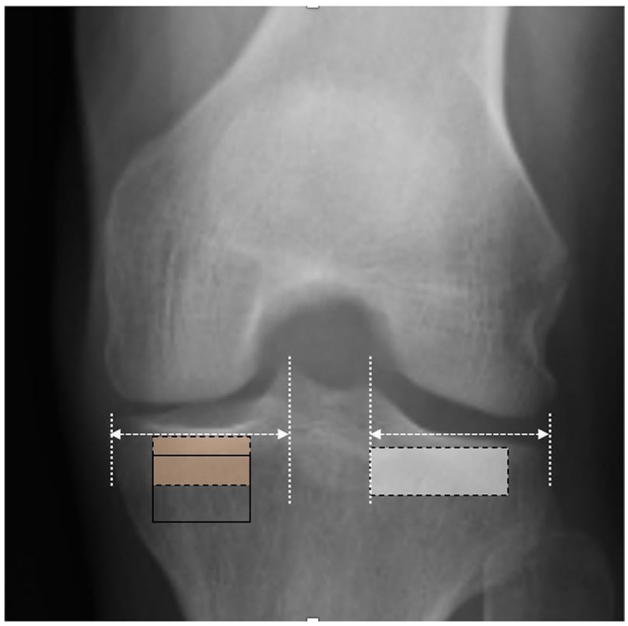

Fig. 3 Various regions of interest (ROI) can be defined to conduct fractal signature analysis. The gray dashed box seen in the lateral tibial compartment defines an ROI of height 6 mm aligned with the lateral tibial plateau and spanning 3/4ths of the length from the lateral tibial plateau to the lateral tibial spine (defined by Kraus et al.) [33]. In the medial tibial compartment, an ROI of height 6 mm and width 14 mm is defined and placed immediately below the cartilage-bone interface in the middle of the distance between the tibial plateau and spine (orange dashed box). A second ROI (transparent box) of height 14 mm and width 14 mm id placed below the dense subchondral bone area. These two medial compartment ROIs have been previously defined by Hirvasniemi et al. [37] (Images and ROIs to scale)

Imaging biomarkers for subchondral bone assessment relevant to OA outcomes

Plain radiography

Fractal signature analysis

Trabecular bone texture (TBT) became a focus of investigation for OA-related subchondral bone architectural changes, such as differences in texture and integrity. The use of TBT calculated by the Fractal signature analysis (FSA) is a technique that can analyze the complexity of subchondral bone structure using a two-dimensional radiographic image (as a projection of the three-dimensional architecture) at a variety of scales spanning the typical size range of trabeculae (100–300 µm) and trabecular spaces (200–2000 µm) (Fig. 3). The subchondral bone architecture is determined by the number, spacing, and cross-connectivity of bone trabeculae [33–35]. The predictive value of FSA of the subchondral bone used for predicting radiographic OA progression was tested by Kraus and colleagues. They demonstrated that FSA of the medial tibial plateau at baseline, derived from analysis of knee X-rays utilizing the Knee Analyzer tool (Optasia Medical, Manchester, UK), was predictive of medial joint space narrowing (mJSN) progression in patients with KL grades 1–3 and thus could be considered as a potential prognostic imaging biomarker of OA at its earlier stages [33]. Kraus et al. further looked at subchondral bone trabecular integrity on plain radiographs. They found that FSA of subchondral trabecular bone integrity could predict MRI measures of OA progression over 12- and 24-month periods [36].

Janvier et al. determined semi-automatic X-ray-derived TBT to be a good predictor of knee OA progression and JSN [38]. The findings of this pilot study indicate that joint unloading implants may alter knee OA progression, defined as changes in JSN, KL grades, and tibial osteophytes, by improving subchondral bone trabecular integrity. The study showed a decrease in fractal signatures of the vertically oriented trabeculae in the medial compartment of the treated knee despite an increase in the untreated knee [39]. Another randomized controlled trial on the structural integrity of the subchondral bone in knee OA showed that patients with marked JSN receiving risedronate (15 mg/day) retained vertical trabecular structure, and those receiving risedronate (50 mg/week) increased vertical trabecular number, both quantified using FSA [40]. Therefore, FSA has been a useful tool for complex measurements of OA-related subchondral bone changes, such as trabecular texture and integrity, through widely used radiographic imaging and demonstrates the potential for providing structural insights for future DMOAD clinical trials.

Computed tomography (CT)

Cone-beam CT (CBCT)

CT studies provide measures of subchondral BMD in knee OA patients, and the use of quantitative CT (QCT) has been shown to provide 1–2% precision in measuring subchondral BMD [41, 42]. As conventional CT scanners have limited spatial resolution compared to that demanded by the small size of trabeculae, trabecular morphometry measurements pose a challenging task for QCT using conventional multidetector CT (MDCT) [43]. The emerging cone-beam CT (CBCT) systems for musculoskeletal (MSK) imaging provide a promising alternative CT technique [44–47]. Their spatial resolution is generally better than in MDCT because CBCT uses flat-panel detectors with smaller pixel sizes (< 200 µm) compared to MDCT detectors. Moreover, the spatial resolution of CBCT is isotropic, i.e., there is no difference between the in-plane and slice directions. The greater resolution of MSK CBCT was shown in a study by Demehri et al., in which the modality was superior to MDCT in image quality of knee examinations for bone visualization tasks, including the trabecular pattern of medullary bone, cortical bone, and fractures detection. [48]. Furthermore, most MSK CBCT scanners are capable of weight-bearing imaging of the lower extremity, thus potentially enabling simultaneous assessment of subchondral bone measures and JSN in OA [48, 49]. Therefore, ongoing efforts aim to establish the feasibility of new CBCT imaging techniques for quantitative assessment of subchondral bone changes in knee OA.

In terms of subchondral bone densitometry, Turunen and colleagues used contrast enhanced-CBCT (CE-CBCT) to obtain volumetric BMD (vBMD) of cortical bone, trabecular bone, subchondral trabecular bone, and subchondral plate in cadaveric specimens and in vivo human volunteers [50]. The vBMD estimates from CE-CBCT were shown to correlate strongly with conventional QCT. In a follow-up study of patients with suspected knee injuries, Myller et al. demonstrated that vBMD and delayed cartilage contrast enhancement by CE-CBCT are related to the severity of cartilage lesions [51].

In terms of macroscale morphological subchondral bone alterations, Segal et al. demonstrated better sensitivity and accuracy of MSK CBCT compared to radiography for the detection of subchondral cysts [52] (Fig. 4). Microscopic quantification of subchondral trabecular bone using MSK CBCT remains primarily in the phase of technical performance assessment. In the study of Guha et al. using distal radius bone samples, an MSK CBCT system (Planmed Verity, Helsinki, Finland) achieved correlations with gold standard µCT of $r = 0.60$ for measurements of trabecular thickness and $r = 0.66$ for trabecular spacing [53]. A new generation of CBCT using the recently introduced fast, low-noise, ultra-high-resolution complementary metal oxide semiconductor and indium gallium zinc oxide flat-panel detectors will likely provide improved trabecular imaging capabilities. For example, Subramanian et al. showed correlations of $r = 0.96$ for trabecular thickness and $r = 0.85$ for trabecular spacing in trabecular subchondral bone cores from the tibia using a prototype complementary metal oxide semiconductor–based MSK CBCT (Fig. 5) [54]. However, the magnitudes of microarchitectural metrics measured in MSK CBCT remain biased compared to µCT because of insufficient spatial resolution, even for the newest detector hardware [53, 54]. Clinical studies are needed to establish whether the strong correlations between CBCT and µCT are sufficient to detect subchondral bone changes associated with early OA.

Micro-CT has been employed in some experimental studies to investigate the therapeutic efficacy of DMOADs on the subchondral bone. The µCT results from an experimental study by Permuy and colleagues suggested that diacerein (cytokine modulator) and hyaluronic acid (cartilage matrix precursor) significantly modified the orientation of the trabecular lattice [5]. Farnaghi et al. have shown that atorvastatin and mitochondria-specific antioxidants can rescue unfavorable subchondral bone changes in animal models of MetS-OA according to µCT results [55]. Furthermore, in a study by Sun and colleagues, the administration of teriparatide to OA models has been found to slow the disruption of subchondral trabecular bone connectivity as measured by µCT examinations [26]. Additionally, according to experimental studies by Hayami et al. and Lindström et al.,

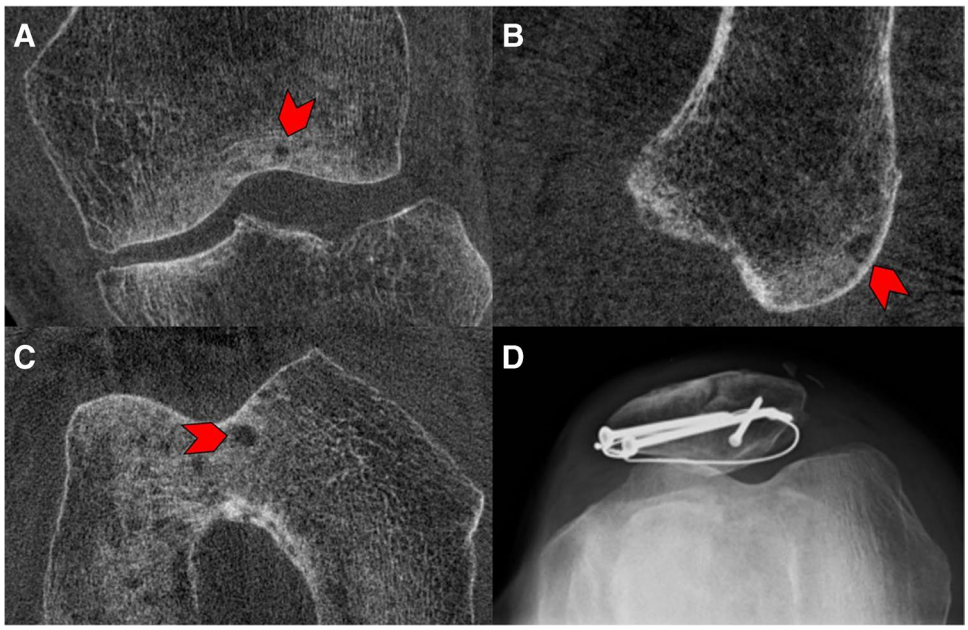

Fig. 4 Images in a 68-year-old male 9 months after open reduction and internal fixation (ORIF) for a patellar fracture. Cone beam computed tomography (CBCT) shows a small subchondral cyst in the coronal (**A**), sagittal (**B**), and axial (**C**) planes (arrowhead). **D** Skyline view radiograph of the same knee demonstrates the hardware used for ORIF. No discrete subchondral cyst is identifiable in the plain radiograph

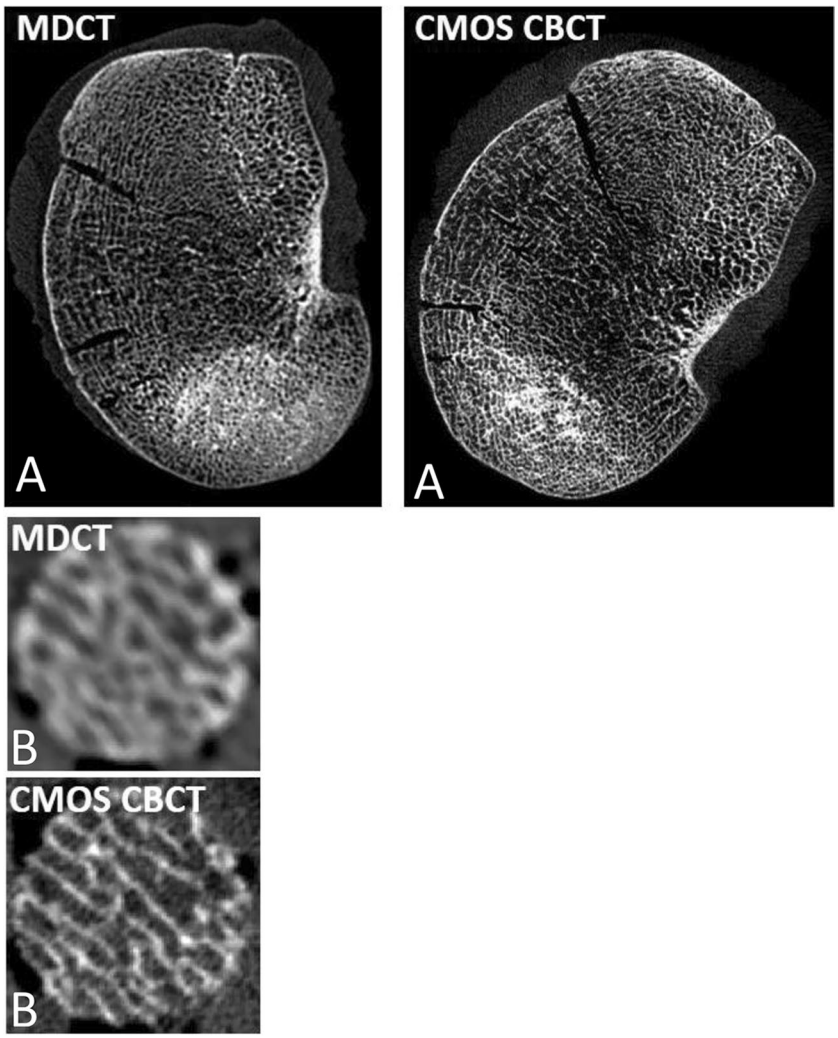

Fig. 5 Comparison of conventional multi-detector computed tomography (MDCT) and musculoskeletal cone-beam computed tomography (CBCT) with a complementary metal oxide semiconductor (CMOS) flat panel detector in visualization of trabecular detail of subchondral bone**: A** Cross-section of a human tibial plateau from a cadaver sample. **B** Cross-sections of a trabecular bone core (~ 8 mm diameter) harvested from underneath tibial plateau. CMOS CBCT image in B is adapted from [54]

it has been demonstrated that cathepsin K inhibitor treatment restores the total thickness of the subchondral bone in animal models of OA based on μCT results [56, 57]. In this context, there is a hope that CBCT with a high resolution approaching μCT could be a potential target for future clinical studies evaluating the DMOAD effect of various drugs on the subchondral bone.

MRI

MOAKS semiquantitative MRI

The MRI osteoarthritis knee score (MOAKS) is an established and validated semi-quantitative scoring system that provides comprehensive and reliable measures of subchondral BMLs, cartilage, and meniscal morphology (Figs. 6, 7 and Table 2) [19]. As an evolution of the Whole Organ Magnetic Resonance Imaging Score and Boston Leeds Osteoarthritis Knee Score, it is one of the most popular and established MRI scoring systems used in large OA observational studies and clinical trials of knee OA and may be used to assess the structural progression of OA longitudinally years after initial diagnosis (Fig. 8) [58].

In 2017, Kogan and colleagues developed a hybrid 3.0 T PET-MRI system, in which they used the MOAKS scoring system to measure biomarkers of OA progression such as BMLs and osteophytes and found that their hybrid system successfully and simultaneously identified morphological (using MRI) and metabolic (using PET) biomarkers of OA progression in early knee OA patients [59]. In a 2020 study, Roemer and colleagues used MOAKS scoring on 3 T MRIs from the Foundation for National Institutes of Health Osteoarthritis Biomarkers Consortium (FNIH, a nested case–control study within the Osteoarthritis Initiative (OAI)) to demonstrate that the subchondral bone phenotype was associated with increased risk of composite (i.e., structural and clinical) progression[58]. Therefore, MOAKS-based structural stratification of knees can be used in patient selection for clinical trials.

MOAKS has also been a valuable tool in assessing the effects of DMOADs on imaging biomarkers of osteoarthritic knees. In a 2020 study, Kon and colleagues used the MOAKS system to evaluate the safety and benefits of using autologous protein solution injections in knee OA patients at baseline and after 24 months. Their results showed that in patients with mild to moderate knee OA and better cartilage status, autologous protein solution injections did not significantly change their OA severity, were safe, and lead to significant pain improvement 3 years after a single injection [60]. Genechten and colleagues aimed to measure the short-term clinical effect, therapeutic response rate, and safety of another injection treatment, namely autologous micro-fragmented adipose tissue injections, and used the MOAKS system to classify mild-to-severe osteoarthritic knees at baseline and up to 12 months [61]. They found that autologous μ-fragmented adipose tissue injections provided early clinical improvement, moderate therapeutic response rate after 12 months, and demonstrated a negative association between MRI-measured BML and therapeutic response rate during this time period [61]. These findings

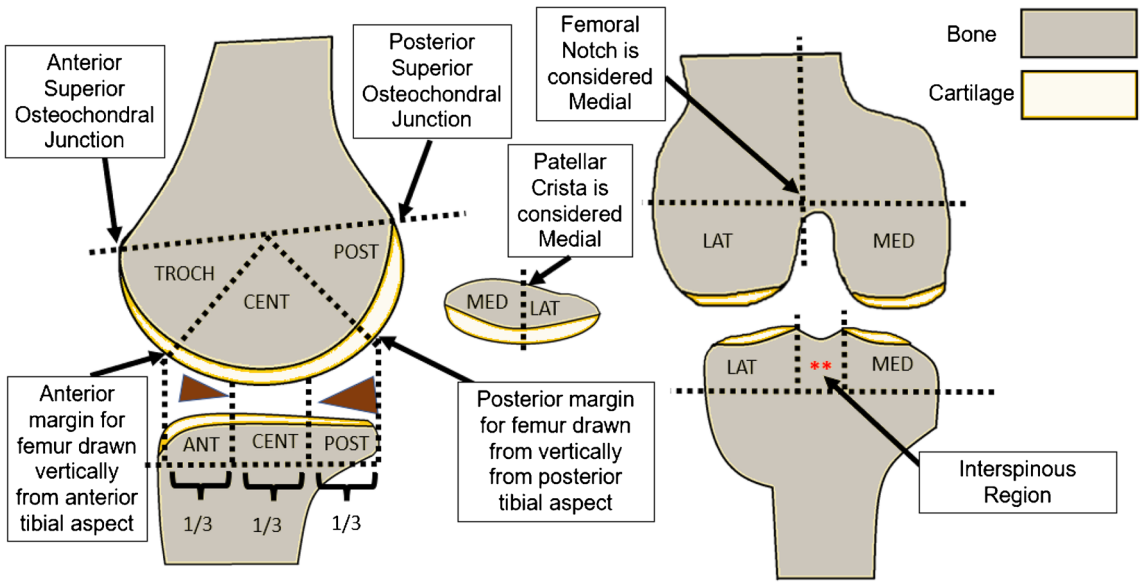

Fig. 6 Schematic illustration showing the 14 segments of evaluation for MRI Osteoarthritis Knee Score (MOAKS). Boundaries of interest have been defined, such as the inclusion the patellar crista in the medial patellar compartment and inclusion of the femoral notch in the medial femoral compartment, respectively. *TROCH* trochlear, *ANT* anterior, *CENT* central, *POST* posterior, *LAT* lateral, *MED* medial

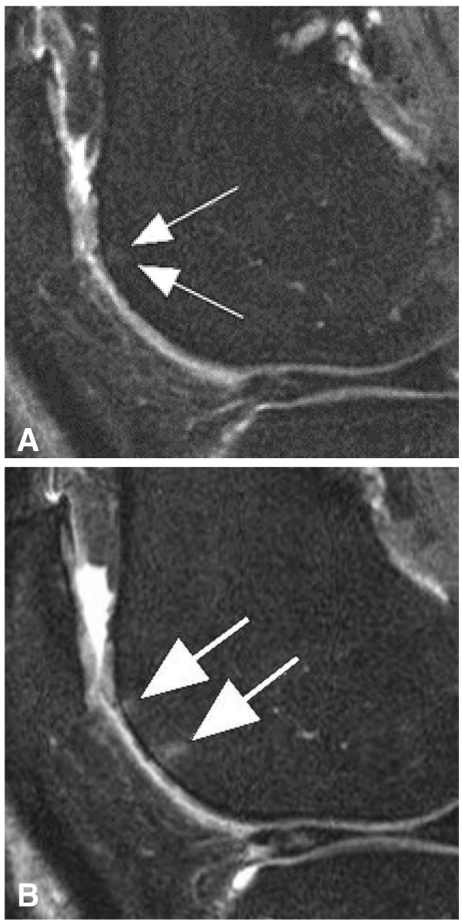

Fig. 7 Bone marrow lesion (BML) incidence: **A** Sagittal intermediate-weighted fat-suppressed magnetic resonance imaging (MRI) scan exhibits a small MRI Osteoarthritis Knee Score (MOAKS)/Whole-Organ MRI Score (WORMS) grade 1 BML in the anterior subregion of the lateral femur (arrows). **B** A follow-up image obtained one year after Fig. 7A. shows a new BML in the same subregion (large arrow) with the initial BML showing a slight increase in size (small arrow). Scoring would reflect a within-grade change of a grade 1 lesion using WORMS and MOAKS. Using MOAKS, the new BML would also be coded as the increase in the number of lesions from 1 to 2. Both lesions are ill-defined (edema-like) and no cystic portions are seen

pointed to the role of increases in therapeutic response rate with autologous μ-fragmented adipose tissue injections in lowering patients' MOAKS-assessed BML associated with OA progression. A randomized clinical trial on 74 subjects with knee OA showed that an intramuscular therapeutic dose of clodronate followed by a maintenance dose is effective for the improvement of BMLs and bone marrow edema, paired without treatment in (Fig. 9), according to the Whole Organ Magnetic Resonance Imaging Score over 12 months (200 mg daily for 15 days and then once weekly for the next 11.5 months) [62].

A study on the longitudinal, multi-center OAI database demonstrated that statin treatment may be protective against the MRI derived OA-related subchondral bone damage in

Table 2 Semi-quantitative MRI scoring osteoarthritis knee score (MOAKS)

Component	Subregions	Score	Description
Bone marrow lesions and cysts	• 2 subregions of patella: medial and lateral patella on axial view • 6 subregions of femur: medial and lateral trochlea, medial and lateral central femur, and the medial and lateral posterior femur • 6 subregions of tibia: medial and lateral tibia (anterior, central, posterior)	0: none 1: < 33% 2: 33–66% 3: > 66%	• Subregional volume of bone marrow lesion (including cysts) in regard to the total volume of the subregion occupied by bone marrow lesion (s) • % of lesion that is bone marrow lesion as distinct from cyst • Number of bone marrow lesions counted

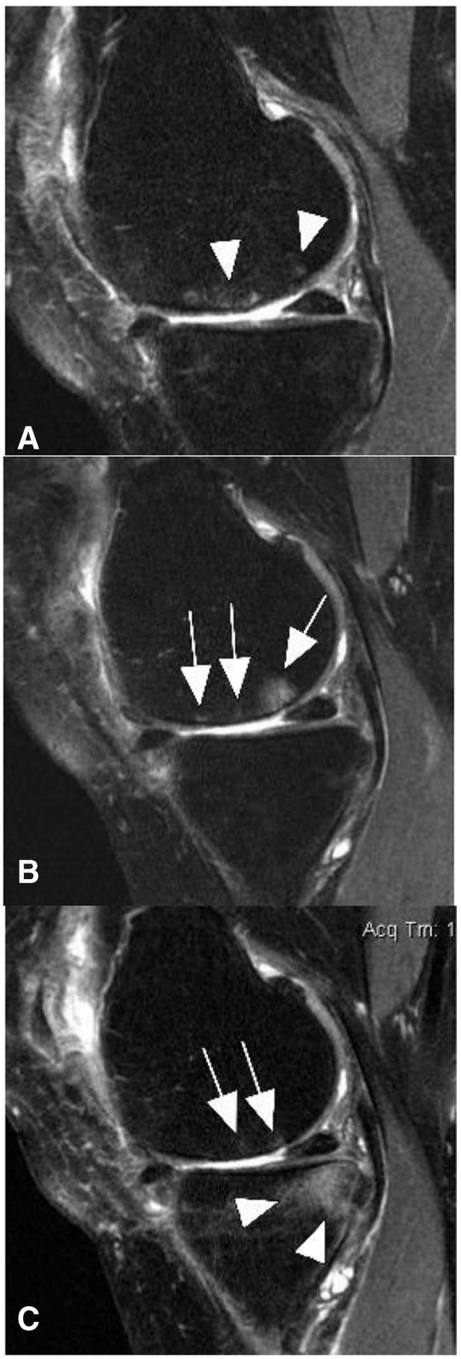

Fig. 8 Bone marrow lesion (BML) assessment over several time points: **A** Baseline sagittal intermediate-weighted fat-suppressed magnetic resonance imaging (MRI) scan exhibits two distinct ill-defined BMLS in the central subregion of the medial femur (arrows). Overall lesion size in subregion qualifies as a grade 1 MRI Osteoarthritis Knee Score (MOAKS)/grade 2 Whole-Organ MRI Score (WORMS) lesion. **B** One year later within-grade increase in overall subregional lesion size in the same central medial femoral subregion is observed. In contrast to Fig. 8A, now there are three distinct lesions that can be differentiated (arrows). The anterior BML has split into two separate lesions with a decrease in lesion size, while the previous posterior lesion exhibits an increase in lesion size. Note, diffuse femoral cartilage loss in addition. **C** Follow-up MRI 2 years after baseline shows a decrease in overall central femoral BML size with now a total subregional score of 1 using both WORMS and MOAKS. There are two distinct lesions now with the most anterior lesion seen in Fig. 8B showing complete regression (small arrows). No cystic component of lesions is observed. There is also a large (grade 3 WORMS and MOAKS) incident lesion in the posterior medial tibia subregion (arrowheads). Without the clinical information, the posterior lesion cannot be further characterized. Traumatic bone contusions, e.g., due to an anterior cruciate ligament tear may exhibit comparable image morphology (reticular pattern with very diffuse borders atypical for OA-associated BMLs). Also, the articular cartilage in the posterior medial tibia is normal, which may further suggest a possible traumatic origin as OA-related BMLs are commonly associated with cartilage damage

a subset of patients who had no/minimal baseline BML, were under statin therapy due to cardiovascular disease, and demonstrated generalized OA phenotype [63]. The effects of zoledronic acid administration on the subchondral bone are controversial in the literature. In a recent 2-year clinical trial, twice-yearly administration of 5 mg of zoledronic acid at baseline and within 12 months showed no significant improvement for MRI-detected BML size in a group of 223 patients [64]. This result contradicted the results of a small pilot trial including 59 individuals, which found that a single dose of zoledronic acid (5 mg) reduced MRI-detected BML size over 6 months [65]. Another 2020 study by Ballal et al. investigated oral treatments for OA using sagittal turbo spin echo fat–suppressed intermediate-weighted MRI of knee OAs in women on an oral bisphosphonate treatment and showed that after comparing BML volume at baseline and after 12 months, the treatment provided no benefit, in terms of changing BML volume, for knee OA patients[66]. In a new, 2022 study by Huang et al., they aimed to use intelligent algorithms, including gray projection algorithms, adaptive binarization algorithms, and active shape models, as a basis for treatment of knee OA with platelet-rich plasma [67]. In their study, they used the MOAKS score and measurements of the inferior angle of the femur, superior angle of the tibia, and tibiofemoral angle by an automatic magnetic resonance diagnostic model to validate the diagnostic findings of the intelligent algorithms and measure the treatment effects of platelet-rich plasma in osteoarthritic knees and found the MOAKS scores of OA patients to be lower after treatment.

In vitro histologic and experimental studies have shown promising results for the DMOAD role of strontium ranelate by inhibition of subchondral bone remodeling [68, 69]. Strontium ranelate has also been demonstrated to improve the joint structure and symptoms of knee OA, however, its impact on subchondral BMLs in clinical practice is not well understood [70, 71]. In a large population of knee OA patients, it was shown that MRI-measured bone marrow abnormalities were positively interrelated with urinary C-telopeptide of type C collagen (CTX-II)

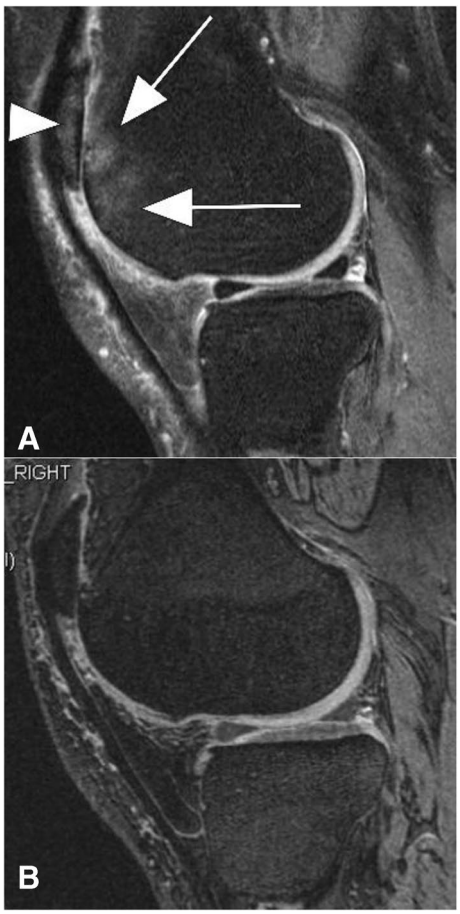

Fig. 9 MRI sequence protocol considerations for bone marrow lesion (BML) assessment: **A** Sagittal intermediate-weighted fat-suppressed magnetic resonance imaging (MRI) scan depicts ill-defined BML in the anterior lateral femur (arrows), reflecting a grade 3 lesion in both systems: MRI Osteoarthritis Knee Score (MOAKS) and Whole-Organ MRI Score (WORMS). In addition, there is a large BML at the lateral patella (arrowhead). **B** Corresponding dual-echo at steady-state (DESS) MRI does not allow differentiation of BML from unaffected marrow due to magnetic susceptibility, despite DESS being a sequence with T2-weighted image characteristics. This low sensitivity for BML detection, especially for edema-like lesions, is the characteristic of all gradient echo sequences, including DESS

as a biomarker of type II collagen degeneration and progression of OA [72]. An early decrease in the level of CTX-II was seen in risedronate-treated patients, but the mechanism is unclear. This may represent a primary effect on subchondral bone turnover leading to improvement in cartilage stability [73].

Despite vitamin D's crucial role in calcium homeostasis, bone metabolism, and subchondral remodeling, to date, original studies and meta-analyses on knee OA MRI have failed to prove the potential role of vitamin D supplementation on subchondral bone structure assessed as improvements in the tibia cartilage volume, JSW, and BMLs [74, 75].

High-resolution three-dimensional (3D) fast MR imaging with free steady-state precession [FISP])

Bolbos et al. used 3 T MRIs of TBT and showed that cartilage degeneration was associated with loss of mineralized subchondral bone [76]. There was an association between the decrease in the MRI-derived subchondral bone quantitative measures and abnormal measures of compositional MRI parameters for early cartilage degeneration such as increased T1rho and T2 relaxation times [76].

MacKay and colleagues further pursued subchondral bone texture analysis using MRI. They used fast imaging with gradient echo (GRE) sequence such as steady-state precession (FISP) to assess the subchondral bone texture of knee joints from the participants of the OAI Bone Ancillary Study at the 30- or 36-month and the 48-month visits and defined OA progression as radiographic medial tibiofemoral joint space width loss between the patients' 36–72-month visits [77]. This study demonstrated the value of MRI-assessed subchondral bone texture as an imaging biomarker for OA progression in clinical trials as the 12–18-month change in subchondral bone architecture was significantly associated with radiographic OA progression at 36 months [77]. The periarticular bone was also quantitatively assessed as a biomarker for early detection of OA progression in a study by Lo and colleagues [78]. Their longitudinal study used 12–18 months of OAI MRI measurements to evaluate OA patients' trabecular bone morphometry, defined as apparent bone volume fraction, trabecular number, thickness, and spacing. The researchers found an association between high progression of JSN with higher MRI-detected baseline measures of the bone volume fraction, trabecular number, and thickness as well as lowered baseline and decreasing trend in trabecular spacing [78]. Therefore, periarticular bone assessments provided an avenue for early detection of OA progression and later prevention of progress.

Pishgar and colleagues attempted to develop a framework for the computer-assisted measurement of trabecular biomarkers and extract subchondral trabecular biomarkers derived from conventional knee MRIs (intermediate-weighted sequences) of patients enrolled in OAI [79]. They extracted the subchondral bone quantitative biomarkers from OAI's Bone Ancillary Study, such as trabecular thickness, spacing, connectivity density, and bone-to-total volume ratio obtained from conventional intermediate-weighted MRI sequences. Out of the evaluated biomarkers, trabecular thickness and bone-to-total volume ratio demonstrated high reliability compared to high-resolution FISP. There was also a modest association with OA progression up to 48 months [79]. Subsequently,

they focused on the trabecular thickness and bone-to-total volume ratio measures from conventional MRI scans of OAI's FNIH OA biomarkers consortium. They demonstrated an association between the evaluated biomarkers and increased medial tibial cartilage volume loss at both the 12-month and 24-month follow-ups [18]. Over the course of these studies, their team suggested the potential value of measuring MRI subchondral trabecular biomarkers from conventional intermediate-weighted sequences to detect structural OA progression as early as 1 year after baseline. Although some high-resolution GRE sequences (e.g., FISP) can depict subchondral trabecular morphometry, other GRE sequences, such as dual-echo at steady-state (DESS), are not suitable for BML detection due to low sensitivity caused by trabecular magnetic susceptibility (Figs. 9, 10) [80].

Other imaging modalities

Bone density scan (DEXA scan)

In addition to "local" subchondral bone analysis in knee OA patients (which is the primary focus of this narrative review), it has been also suggested in the literature that OA and "systemic" osteoporosis are negatively associated as they uncommonly occur simultaneously. Despite decades of research, the exact association pattern and underlying mediatory factors between systemic/local BMD and the incidence/progression of OA remain unclear. A prospective cohort of 86 subjects with symptomatic knee OA showed that BMD of the hip was negatively associated with cartilage damage and subchondral BMLs [81], and another prospective cohort of 153 subjects without clinical OA demonstrated that higher systemic BMD was associated with increased early knee cartilage damage [82]. In a prospective cohort of 158 subjects, DEXA-derived systemic BMD was positively associated with increased cartilage thickness in patients with radiographic OA using both cross-sectional and longitudinal analysis [83]. Additionally, high medial tibial subchondral BMD predicted an increase in medial tibial cartilage thickness longitudinally over the period of 2.7 years [83]. Further studies are warranted to reveal the mechanism of subchondral BMD changes using DEXA in the setting of knee OA, which may prove helpful in the development of DMOADs.

PET

PET imaging can offer a shift of focus on subchondral bone imaging biomarkers from quantitative structural biomarkers to those reflecting changes in subchondral bone metabolism related to knee OA pathogenesis. Using a 3 T hybrid PET/MRI system, Watkins et al. found that bone perfusion, tracer extraction fraction, and total tracer uptake into bone significantly differed in knee OAs [84]. These findings suggest that subchondral bone metabolism is altered in knee OA and provide a tool to further explore the subchondral bone during the initiation and progression of OA [84]. Subsequently, Jena et al. continued this examination of [18F] NaF uptake using hybrid PET/MRI systems in a series of case studies of patients with varying OA severity (KL grades 1–4) and also suggested the distinct value of PET for subchondral bone analysis in future DMOAD clinical trials [85].

Artificial intelligence for the assessment of subchondral bone

Exponential increases in the use of artificial intelligence (AI) in evaluation of knee OA can provide a venue for automated and rapid prediction of disease outcomes and progression in the research setting. A recent study by Almhdie-Imjabbar et al. builds on imaging studies that had identified TBT as an imaging biomarker for OA progression and introduces using AI on conventional radiographs to provide prognostic data for knee OA outcomes [38, 86].

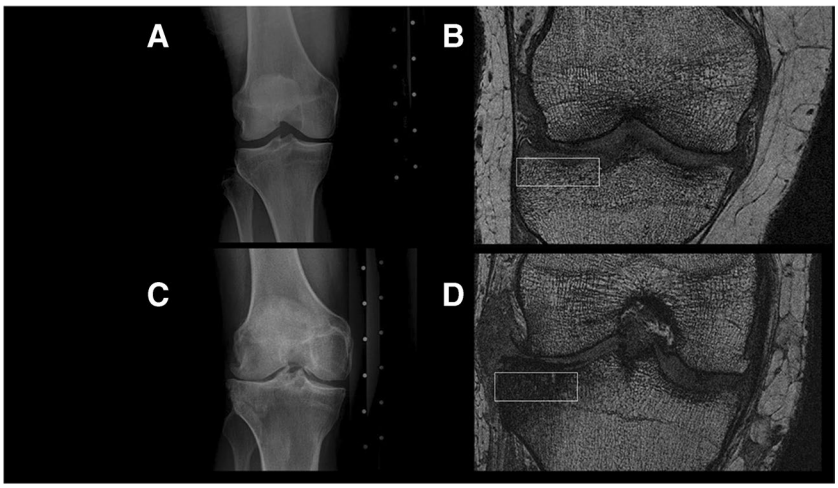

Fig. 10 **A** Radiograph showing a normal knee joint with Kellgren-Lawrence grade 0. **B** Fast imaging with steady state precession (FISP) sequence MRI acquisition shows normal subchondral trabecular morphometry. **C** Radiograph of a knee with marked narrowing of the lateral joint space (Kellgren-Lawrence grade 4) **D** FISP sequence MRI acquisition of the same diseased joint shows altered subchondral trabecular morphometry in the lateral tibial plateau

They used data from the OAI and Multicenter Osteoarthritis Study cohorts and automatically segmented subregions of interest from the plain radiographs of patients with KL grades 2–3. In both cohorts, OA progression was defined as mJSN increases during the follow-up radiographic examinations. Akin to FSA, subchondral bone texture analysis using TBT-convolutional neural networks (TBT-CNN) predicted mJSN in OA patients over a period of 4–6 years [86]. Such algorithm-based subchondral texture analysis has also been recently used to automatically quantify structural changes induced by DMOADs. A 2022 study by Jang and colleagues used a fully automated AI algorithm model to analyze the changes in the upper tibial subchondral bone structure measures in patients undergoing polynucleotide filler injections (HP cell Vitaran J) once a week for 5 weeks [87]. They found that the patients' Visual Analogue Scale and WOMAC decreased for 3 months after polynucleotide treatment and that AI-detected changes in their subchondral bone texture analysis measures [87]. Overall, these findings demonstrate that AI can be a valuable tool for automated detection of microstructural changes in the subchondral bone and may be used to asses therapeutic strength of DMOADs in future clinical trials.

Conclusions

The subchondral bone has been shown to be a possible target for secondary preventive measures of knee OA including future potential DMOAD developments and assessments. Fractal signature analysis with radiography has helped model and quantitatively measure subchondral bone microarchitecture while serving as a tool to predict trabecular texture and integrity as predictive measures of OA progression. New developments in CT techniques, such as CBCT and CE-CBCT with an improved spatial resolution for bone imaging, can tremendously impact OA diagnosis and outcome prediction. MRI has been tremendously implemented for subchondral bone analysis in knee OA patients, including BML (using the semiquantitative MOAKS and quantitative assessment), subchondral trabecular bone morphometry measurements, and TBT (using TrueFISP). DEXA scans provide BMD measurements which can be used to predict changes in subchondral BMLs, cartilage degeneration, and OA progression. PET scans can also provide quantitative measurements related to subchondral bone physiology and aid in the understanding of OA initiation and progression. AI is an exponentially expanding research focus in subchondral bone imaging research, which aims at automating TBT analysis and OA prediction. Despite the lack of pharmacological treatment for OA, familiarity with various available and advanced imaging modalities will certainly help in optimizing the imaging protocols for assessment of potential DMOADs and their protective effect on knee OA in future clinical investigations.

Declarations

Conflict of interest This study received support from the R01AR079620-01 award, with Shadpour Demehri being the recipient of the award. Other authors declare no other conflicts of interest.

References

1. Cui A, Li H, Wang D, Zhong J, Chen Y, Lu H. Global, regional prevalence, incidence and risk factors of knee osteoarthritis in population-based studies. EClinicalMedicine. 2020;29–30:100587.
2. Safiri S, Kolahi A-A, Smith E, Hill C, Bettampadi D, Mansournia MA, et al. Global, regional and national burden of osteoarthritis 1990–2017: a systematic analysis of the Global Burden of Disease Study 2017. Ann Rheum Dis. 2020;79:819–28.
3. Chu CR, Williams AA, Coyle CH, Bowers ME. Early diagnosis to enable early treatment of pre-osteoarthritis. Arthritis Res Ther. 2012;14:212.
4. Sovani S, Grogan SP. Osteoarthritis. Orthop Nurs. 2013;32:25–36.
5. Permuy M, Guede D, López-Peña M, Muñoz F, Caeiro J-R, González-Cantalapiedra A. Comparison of various SYSADOA for the osteoarthritis treatment: an experimental study in rabbits. BMC Musculoskelet Disord. 2015;16:120.
6. Salazar J, Bello L, Chávez M, Añez R, Rojas J, Bermúdez V. Glucosamine for osteoarthritis: biological effects, clinical Efficacy, and safety on glucose metabolism. Arthritis. 2014;2014:1–13.
7. Deveza LA, Loeser RF. Is osteoarthritis one disease or a collection of many? Rheumatology. 2018;57:iv34-42.
8. Goldring MB, Goldring SR. Articular cartilage and subchondral bone in the pathogenesis of osteoarthritis. Ann N Y Acad Sci. 2010;1192:230–7.
9. Mohajer B, Dolatshahi M, Moradi K, Najafzadeh N, Eng J, Zikria B, et al. Role of thigh muscle changes in knee osteoarthritis outcomes: Osteoarthritis Initiative data. Radiology. 2022;305:169–78.
10. Mohajer B, Moradi K, Guermazi A, et al. Diabetes-associated thigh muscle degeneration mediates knee osteoarthritis-related outcomes: results from a longitudinal cohort study. Eur Radiol. 2023;33(1):595–605.
11. Lories RJ, Luyten FP. The bone-cartilage unit in osteoarthritis. Nat Rev Rheumatol. 20101207th ed. 2011;7:43–9.
12. Buckland-Wright C. Subchondral bone changes in hand and knee osteoarthritis detected by radiography. Osteoarthr Cartil. 2004;12:10–9.
13. Castañeda S, Roman-Blas JA, Largo R, Herrero-Beaumont G. Subchondral bone as a key target for osteoarthritis treatment. Biochem Pharmacol. 2012;83:315–23.
14. Javaid MK, Arden NK. Bone and osteoarthritis: what is the relationship? Arthritis Rheum. 2013;65:1418–20.
15. Baker-LePain JC, Lane NE. Role of bone architecture and anatomy in osteoarthritis. Bone. 2012;51:197–203.
16. Wluka AE, Wang Y, Davies-Tuck M, English DR, Giles GG, Cicuttini FM. Bone marrow lesions predict progression of

cartilage defects and loss of cartilage volume in healthy middle-aged adults without knee pain over 2 yrs. Rheumatology. 2008;47:1392–6.
17. Felson DT, Chaisson CE, Hill CL, Totterman SMS, Gale ME, Skinner KM, et al. The Association of Bone Marrow Lesions with Pain in Knee Osteoarthritis. Ann Intern Med. 2001;134:541.
18. Pishgar F, Ashraf-ganjouei A, Dolatshahi M, Guermazi A, Zikria B, Cao X, et al. Conventional MRI-derived subchondral trabecular biomarkers and their association with knee cartilage volume loss as early as 1 year: a longitudinal analysis from Osteoarthritis Initiative. Skeletal Radiol. 2022;51:1959–66.
19. Hunter DJ, Guermazi A, Lo GH, Grainger AJ, Conaghan PG, Boudreau RM, et al. Evolution of semi-quantitative whole joint assessment of knee OA: MOAKS (MRI Osteoarthritis Knee Score). Osteoarthr Cartil. 2011;19:990–1002.
20. Neogi T, Bowes MA, Niu J, de Souza KM, Vincent GR, Goggins J, et al. Magnetic resonance imaging-based three-dimensional bone shape of the knee predicts onset of knee osteoarthritis: data from the Osteoarthritis Initiative. Arthritis Rheum. 2013;65:2048–58.
21. Weinans H, Siebelt M, Agricola R, Botter SM, Piscaer TM, Waarsing JH. Pathophysiology of peri-articular bone changes in osteoarthritis. Bone. 2012;51:190–6.
22. Zhen G, Wen C, Jia X, Li Y, Crane JL, Mears SC, et al. Inhibition of TGF-β signaling in mesenchymal stem cells of subchondral bone attenuates osteoarthritis. Nat Med. 2013;19:704–12.
23. Mapp PI, Walsh DA. Mechanisms and targets of angiogenesis and nerve growth in osteoarthritis. Nat Rev Rheumatol. 2012;8:390–8.
24. Burr DB, Gallant MA. Bone remodelling in osteoarthritis. Nat Rev Rheumatol. 2012;8:665–73.
25. Su W, Liu G, Liu X, Zhou Y, Sun Q, Zhen G, et al. Angiogenesis stimulated by elevated PDGF-BB in subchondral bone contributes to osteoarthritis development. JCI Insight. 2020;5.
26. Sun Q, Zhen G, Li TP, Guo Q, Li Y, Su W. Parathyroid hormone attenuates osteoarthritis pain by remodeling subchondral bone in mice. eLife. 2021;10:e66532.
27. Su W, Liu G, Mohajer B, Wang J, Shen A, Zhang W, et al. Senescent preosteoclast secretome promotes metabolic syndrome associated osteoarthritis through cyclooxygenase 2. Elife. 2022;11.
28. Jeon OH, Kim C, Laberge R-M, Demaria M, Rathod S, Vasserot AP, et al. Local clearance of senescent cells attenuates the development of post-traumatic osteoarthritis and creates a pro-regenerative environment. Nat Med. 2017;23:775–81.
29. Jeon OH, David N, Campisi J, Elisseeff JH. Senescent cells and osteoarthritis: a painful connection. J Clin Investig. 2018;128:1229–37.
30. Bailey KN, Nguyen J, Yee CS, Dole NS, Dang A, Alliston T. Mechanosensitive control of articular cartilage and subchondral bone homeostasis in mice requires osteocytic transforming growth factor β signaling. Arthritis Rheumatol. 2021;73:414–25.
31. Bouaziz W, Funck-Brentano T, Lin H, Marty C, Ea H-K, Hay E, et al. Loss of sclerostin promotes osteoarthritis in mice via β-catenin-dependent and -independent Wnt pathways. Arthritis Res Ther. 2015;17:24.
32. Funck-Brentano T, Bouaziz W, Marty C, Geoffroy V, Hay E, Cohen-Solal M. Dkk-1-mediated inhibition of Wnt signaling in bone ameliorates osteoarthritis in mice. Arthritis Rheumatol. 2014;66:3028–39.
33. Kraus VB, Feng S, Wang S, White S, Ainslie M, Brett A, et al. Trabecular morphometry by fractal signature analysis is a novel marker of osteoarthritis progression. Arthritis Rheum. 2009;60:3711–22.
34. Lynch JA, Hawkes DJ, Buckland-Wright JC. A robust and accurate method for calculating the fractal signature of texture in macroradiographs of osteoarthritic knees. Med Inform. 1991;16:241–51.
35. Lynch JA, Hawkes DJ, Buckland-Wright JC. Analysis of texture in macroradiographs of osteoarthritic knees, using the fractal signature. Phys Med Biol. 1991;36:709–22.
36. Kraus VB, Feng S, Wang S, White S, Ainslie M, Le Graverand M-PH, et al. Subchondral bone trabecular integrity predicts and changes concurrently with radiographic and magnetic resonance imaging-determined knee osteoarthritis progression. Arthritis Rheum. 2013;65:1812–21.
37. Hirvasniemi J, Thevenot J, Multanen J, Haapea M, Heinonen A, Nieminen MT, et al. Association between radiography-based subchondral bone structure and MRI-based cartilage composition in postmenopausal women with mild osteoarthritis. Osteoarthr Cartil. 2017;25:2039–46.
38. Janvier T, Jennane R, Valery A, Harrar K, Delplanque M, Lelong C, et al. Subchondral tibial bone texture analysis predicts knee osteoarthritis progression: data from the Osteoarthritis Initiative. Osteoarthr Cartil. 2017;25:259–66.
39. Miller L, Sode M, Fuerst T, Block J. Joint unloading implant modifies subchondral bone trabecular structure in medial knee osteoarthritis: 2-year outcomes of a pilot study using fractal signature analysis. Clin Interv Aging. 2015;351.
40. Buckland-Wright JC, Messent EA, Bingham CO, Ward RJ, Tonkin C. A 2 yr longitudinal radiographic study examining the effect of a bisphosphonate (risedronate) upon subchondral bone loss in osteoarthritic knee patients. Rheumatology. 2006;46:257–64.
41. Johnston JD, Masri BA, Wilson DR. Computed tomography topographic mapping of subchondral density (CT-TOMASD) in osteoarthritic and normal knees: methodological development and preliminary findings. Osteoarthr Cartil. 2009;17:1319–26.
42. Bousson V, Lowitz T, Laouisset L, Engelke K, Laredo J-D. CT imaging for the investigation of subchondral bone in knee osteoarthritis. Osteoporos Int. 2012;23:861–5.
43. Griffith JF, Genant HK. New imaging modalities in bone. Curr Rheumatol Rep. 2011;13:241–50.
44. Zbijewski W, de Jean P, Prakash P, Ding Y, Stayman JW, Packard N, et al. A dedicated cone-beam CT system for musculoskeletal extremities imaging: Design, optimization, and initial performance characterization. Med Phys. 2011;38:4700–13.
45. Tuominen EKJ, Kankare J, Koskinen SK, Mattila KT. Weight-bearing CT imaging of the lower extremity. Am J Roentgenol. 2013;200:146–8.
46. Carrino JA, Al Muhit A, Zbijewski W, Thawait GK, Stayman JW, Packard N, et al. Dedicated cone-beam CT system for extremity imaging. Radiology. 2014;270:816–24.
47. Huang AJ, Chang CY, Thomas BJ, MacMahon PJ, Palmer WE. Using cone-beam CT as a low-dose 3D imaging technique for the extremities: initial experience in 50 subjects. Skeletal Radiol. 2015;44:797–809.
48. Demehri S, Muhit A, Zbijewski W, Stayman JW, Yorkston J, Packard N, et al. Assessment of image quality in soft tissue and bone visualization tasks for a dedicated extremity cone-beam CT system. Eur Radiol. 2015;25:1742–51.
49. Segal NA, Frick E, Duryea J, Roemer F, Guermazi A, Nevitt MC, et al. Correlations of medial joint space width on fixed-flexed standing computed tomography and radiographs with cartilage and meniscal morphology on magnetic resonance imaging. Arthritis Care Res (Hoboken). 2016;68:1410–6.
50. Turunen MJ, Toyras J, Kokkonen HT, Jurvelin JS. Quantitative evaluation of knee subchondral bone mineral density using cone beam computed tomography. IEEE Trans Med Imaging. 2015;34:2186–90.
51. Myller KAH, Turunen MJ, Honkanen JTJ, Väänänen SP, Iivarinen JT, Salo J, et al. In vivo contrast-enhanced cone beam CT provides quantitative information on articular cartilage and subchondral bone. Ann Biomed Eng. 2017;45:811–8.

52. Segal NA, Nevitt MC, Lynch JA, Niu J, Torner JC, Guermazi A. Diagnostic performance of 3D standing CT imaging for detection of knee osteoarthritis features. Phys Sportsmed. 2015;43:213–20.
53. Guha I, Klintström B, Klintström E, Zhang X, Smedby Ö, Moreno R, et al. A comparative study of trabecular bone microstructural measurements using different CT modalities. Phys Med Biol. 2020;65:235029.
54. Subramanian S, Brehler M, Cao Q, et al. Quantitative evaluation of bone microstructure using high-resolution extremity cone-beam CT with a CMOS detector. Proc SPIE Int Soc Opt Eng. 2019;10953:1095317.
55. Farnaghi S, Prasadam I, Cai G, Friis T, Du Z, Crawford R, et al. Protective effects of mitochondria-targeted antioxidants and statins on cholesterolinduced osteoarthritis. FASEB J. 2017;31:356–67.
56. Hayami T, Zhuo Y, Wesolowski GA, Pickarski M, Duong LT. Inhibition of cathepsin K reduces cartilage degeneration in the anterior cruciate ligament transection rabbit and murine models of osteoarthritis. Bone. 2012;50:1250–9.
57. Lindström E, Rizoska B, Tunblad K, Edenius C, Bendele AM, Maul D, et al. The selective cathepsin K inhibitor MIV-711 attenuates joint pathology in experimental animal models of osteoarthritis. J Transl Med. 2018;16:56.
58. Roemer FW, Collins JE, Neogi T, Crema MD, Guermazi A. Association of knee OA structural phenotypes to risk for progression: a secondary analysis from the Foundation for National Institutes of Health Osteoarthritis Biomarkers study (FNIH). Osteoarthr Cartil. 2020;28:1220–8.
59. Kogan F, Fan AP, McWalter EJ, Oei EHG, Quon A, Gold GE. PET/MRI of metabolic activity in osteoarthritis: a feasibility study. J Magn Reson Imaging. 2017;45:1736–45.
60. Kon E, Engebretsen L, Verdonk P, Nehrer S, Filardo G. Autologous protein solution injections for the treatment of knee osteoarthritis: 3-year results. Am J Sports Med. 2020;48:2703–10.
61. van Genechten W, Vuylsteke K, Martinez PR, Swinnen L, Sas K, Verdonk P. Autologous micro-fragmented adipose tissue (MFAT) to treat symptomatic knee osteoarthritis: early outcomes of a consecutive case series. J Clin Med. 2021;10:2231.
62. Frediani B, Toscano C, Falsetti P, Nicosia A, Pierguidi S, Migliore A, et al. Intramuscular clodronate in long-term treatment of symptomatic knee osteoarthritis: a randomized controlled study. Drugs R D. 2020;20:39–45.
63. Mohajer B, Guermazi A, Conaghan PG, Berenbaum F, Roemer FW, Haj-Mirzaian A, et al. Statin use and MRI subchondral bone marrow lesion worsening in generalized osteoarthritis: longitudinal analysis from Osteoarthritis Initiative data. Eur Radiol. 2022;32:3944–53.
64. Cai G, Aitken D, Laslett LL, Pelletier J-P, Martel-Pelletier J, Hill C, et al. Effect of intravenous zoledronic acid on tibiofemoral cartilage volume among patients with knee osteoarthritis with bone marrow lesions. JAMA. 2020;323:1456.
65. Laslett LL, Doré DA, Quinn SJ, Boon P, Ryan E, Winzenberg TM, et al. Zoledronic acid reduces knee pain and bone marrow lesions over 1 year: a randomised controlled trial. Ann Rheum Dis. 2012;71:1322–8.
66. Ballal P, Sury M, Lu N, Duryea J, Zhang Y, Ratzlaff C, et al. The relation of oral bisphosphonates to bone marrow lesion volume among women with osteoarthritis. Osteoarthr Cartil. 2020;28:1325–9.
67. Huang B, Huang Y, Ma X, Chen Y. Intelligent algorithm-based magnetic resonance for evaluating the effect of platelet-rich plasma in the treatment of intractable pain of knee arthritis. Contrast Media Mol Imaging. 2022;2022:1–11.
68. Tat SK, Pelletier J-P, Mineau F, Caron J, Martel-Pelletier J. Strontium ranelate inhibits key factors affecting bone remodeling in human osteoarthritic subchondral bone osteoblasts. Bone. 2011;49:559–67.
69. Yu D, Ding H, Mao Y, Liu M, Yu B, Zhao X, et al. Strontium ranelate reduces cartilage degeneration and subchondral bone remodeling in rat osteoarthritis model. Acta Pharmacol Sin. 2013;34:393–402.
70. Lafeber FPJG, van Laar JM. Strontium ranelate: ready for clinical use as disease-modifying osteoarthritis drug? Ann Rheum Dis. 2013;72:157–61.
71. Reginster J-Y, Badurski J, Bellamy N, Bensen W, Chapurlat R, Chevalier X, et al. Efficacy and safety of strontium ranelate in the treatment of knee osteoarthritis: results of a double-blind, randomised placebo-controlled trial. Ann Rheum Dis. 2013;72:179–86.
72. Garnero P, Peterfy C, Zaim S, Schoenharting M. Bone marrow abnormalities on magnetic resonance imaging are associated with type II collagen degradation in knee osteoarthritis: a three-month longitudinal study. Arthritis Rheum. 2005;52:2822–9.
73. Bingham CO, Buckland-Wright JC, Garnero P, Cohen SB, Dougados M, Adami S, et al. Risedronate decreases biochemical markers of cartilage degradation but does not decrease symptoms or slow radiographic progression in patients with medial compartment osteoarthritis of the knee: results of the two-year multinational knee osteoarthritis structural arthritis study. Arthritis Rheum. 2006;54:3494–507.
74. Perry TA, Parkes MJ, Hodgson R, Felson DT, O'Neill TW, Arden NK. Effect of vitamin D supplementation on synovial tissue volume and subchondral bone marrow lesion volume in symptomatic knee osteoarthritis. BMC Musculoskelet Disord. 2019;20:76.
75. Zhao Z-X, He Y, Peng L-H, Luo X, Liu M, He C-S, et al. Does vitamin D improve symptomatic and structural outcomes in knee osteoarthritis? A systematic review and meta-analysis. Aging Clin Exp Res. 2021;33:2393–403.
76. Bolbos RI, Zuo J, Banerjee S, Link TM, Benjamin Ma C, Li X, et al. Relationship between trabecular bone structure and articular cartilage morphology and relaxation times in early OA of the knee joint using parallel MRI at 3T. Osteoarthr Cartil. 2008;16:1150–9.
77. MacKay JW, Kapoor G, Driban JB, Lo GH, McAlindon TE, Toms AP, et al. Association of subchondral bone texture on magnetic resonance imaging with radiographic knee osteoarthritis progression: data from the Osteoarthritis Initiative Bone Ancillary Study. Eur Radiol. 2018;28:4687–95.
78. Lo GH, Schneider E, Driban JB, Price LL, Hunter DJ, Eaton CB, et al. Periarticular bone predicts knee osteoarthritis progression: data from the Osteoarthritis Initiative. Semin Arthritis Rheum. 2018;48:155–61.
79. Pishgar F, Guermazi A, Roemer FW, Link TM, Demehri S. Conventional MRI-based subchondral trabecular biomarkers as predictors of knee osteoarthritis progression: data from the Osteoarthritis Initiative. Eur Radiol. 2021;31:3564–73.
80. Walsh DA, Sofat N, Guermazi A, Hunter DJ. Osteoarthritis bone marrow lesions. Osteoarthritis Cartilage. 2022.
81. Teichtahl AJ, Wang Y, Wluka AE, Strauss BJ, Proietto J, Dixon JB, et al. Associations between systemic bone mineral density and early knee cartilage changes in middle-aged adults without clinical knee disease: a prospective cohort study. Arthritis Res Ther. 2017;19:98.
82. Zhu Q, Xu J, Wang K, Cai J, Wu J, Ren J, et al. Associations between systemic bone mineral density, knee cartilage defects and bone marrow lesions in patients with knee osteoarthritis. Int J Rheum Dis. 2018;21:1202–10.
83. Cao Y, Stannus OP, Aitken D, Cicuttini F, Antony B, Jones G, et al. Cross-sectional and longitudinal associations between systemic, subchondral bone mineral density and knee cartilage thickness in older adults with or without radiographic osteoarthritis. Ann Rheum Dis. 2014;73:2003–9.

84. Watkins L, MacKay J, Haddock B, Mazzoli V, Uhlrich S, Gold G, et al. Assessment of quantitative [18F]Sodium fluoride PET measures of knee subchondral bone perfusion and mineralization in osteoarthritic and healthy subjects. Osteoarthr Cartil. 2021;29:849–58.
85. Jena A, Goyal N, Vaishya R. 18F–NaF simultaneous PET/MRI in osteoarthritis: initial observations with case illustration. J Clin Orthop Trauma. 2021;22:101569.
86. Almhdie-Imjabbar A, Nguyen K-L, Toumi H, Jennane R, Lespessailles E. Prediction of knee osteoarthritis progression using radiological descriptors obtained from bone texture analysis and Siamese neural networks: data from OAI and MOST cohorts. Arthritis Res Ther. 2022;24:66.
87. Jang JY, Kim JH, Kim MW, Kim SH, Yong SY. Study of the efficacy of artificial intelligence algorithm-based analysis of the functional and anatomical improvement in polynucleotide treatment in knee osteoarthritis patients: a prospective case series. J Clin Med. 2022;11:2845.